THE ASTROPHYSICAL JOURNAL, 563:597–610, 2001 December 20

X-RAY DESTRUCTION OF DUST ALONG THE LINE OF SIGHT TO γ-RAY BURSTS

ANDREW FRUCHTER
Space Telescope Science Institute, Baltimore, MD 21218
JULIAN H. KROLIK
Department of Physics and Astronomy, Johns Hopkins University, Baltimore, MD 21218
AND
JAMES E. RHOADS
Space Telescope Science Institute, Baltimore, MD 21218
Received 2000 August 4; accepted 2001 July 28

ABSTRACT

We show that if all γ-ray bursts emit X-rays in a way similar to those observed by *BeppoSAX*, much of the extinction along the line of sight in the host galaxy of the burst can be destroyed. Two mechanisms are principally responsible for dust destruction: grain heating and grain charging. The latter, which can lead to electrostatic stresses greater than the tensile strength of the grains, is often the more important. Grains may regularly be destroyed at distances as large as ~ 100 pc. This dust destruction can permit us to see the UV/optical afterglow even when the burst is embedded deep within a highly obscured region. Because the destruction rate depends on grain composition and size, it may be possible to observe the amount and wavelength dependence of extinction change during the course of the burst and first few minutes of the afterglow. It may also be possible to detect interstellar absorption lines in the afterglow spectrum that would not exist but for the return of heavy elements to the gas phase.

Subject heading: gamma rays: bursts

1. INTRODUCTION

Afterglows currently afford the best available diagnostics of γ-ray burst (GRB) environments. Although so far only afterglows from long, soft bursts—a subclass containing about two-thirds of GRBs (Kouveliotou et al. 1993)—have been localized, these localizations have resulted in redshift measurements of the bursts (e.g., Metzger et al. 1997), as well as (subarcsecond) burst positions, and identification and studies of the host galaxies (Hogg & Fruchter 1998; Mao & Mo 1998; Fruchter et al. 1999; Bloom et al. 1999a). One of the most revealing results from afterglow studies is a range of observations possibly suggesting that γ-ray bursts are associated with massive star formation and the associated regions of dense interstellar gas:

1. Host galaxies of γ-ray bursts show systematically blue broadband colors (Fruchter et al. 1999).
2. A number of host galaxies show unusually strong [O II] emission (Bloom et al. 1998; Djorgovski et al. 1998; Vreeswijk et al. 2001).
3. The wide range of optical–to–γ-ray flux ratios may be explained if there is substantial extinction along the line of sight to some bursts. The best documented case here is GRB 970828 (Groot et al. 1997), for which an extreme γ-ray–to–optical ratio was combined with evidence of soft X-ray absorption, suggesting a large column density of interstellar medium (ISM) at a substantial redshift.
4. Features in the light curves and color evolution of GRBs 980326 and 970228 have been interpreted at least by some (Bloom et al. 1999b; Galama et al. 2000) as evidence for associated supernovae, again suggesting a link between GRBs and the deaths of stars sufficiently massive to remain near their natal star forming regions throughout their lives.
5. The peculiar spectral energy distribution of the GRB 980329 afterglow (Fruchter 1999; Reichart et al. 1999) may be due to absorption bands of excited molecular hydrogen in the vicinity of the burster (Draine 1999). This would require a considerable column density of molecular hydrogen ($\sim 10^{18}$ cm^{-2}) in the neighborhood of the burster.
6. Although the measured extinction of the optical transient associated with GRB 980703 is not particularly high ($A_V = 1.5 \pm 0.11$ mag), the low-energy X-ray spectrum of the afterglow is best fit by $N_{\rm H} = 3.6^{+2.2}_{-1.3} \times 10^{22}$ cm^{-3}, which suggests that the burst may nonetheless have occurred in a molecular cloud (Vreeswijk et al. 1999). Other bursts may be similar to GRB 980703 in this regard (Galama & Wijers 2000).

All of these lines of evidence, then, point to a possible association of at least the long duration, soft spectrum bursts with the dense ISM and, hence, with potentially high dust column densities. If large dust column densities are common, then a large fraction of afterglows could be obscured at optical through soft X-ray wavelengths. However, many afterglows—a majority of those observed at optical wavelengths—are in fact relatively blue in their optical colors.

The association of GRBs with star formation may be best reconciled with observed blue colors if GRBs destroy much of the dust along the line of sight to the burst. GRBs are extremely energetic events at all wavelengths, making many dust destruction mechanisms possible. Waxman & Draine (2000) were the first to explore some of these mechanisms in detail. They examined particularly the evaporation of dust grains through direct heating by UV radiation and (more briefly) destruction through photoelectric grain charging. Using a reverse shock model, they scaled the prompt UV/optical emission of GRBs from the single detection of prompt optical emission to date (GRB 990123; Akerlof et al. 1999), which now appears to have been exceptional in its optical and ultraviolet emission (e.g., Williams et al. 1999; Akerlof et al. 2000).

In the present paper, we examine grain evaporation through heating by X-rays, which can dominate over the

heating by UV photons, and also give a more detailed treatment of grain shattering by photoelectric charging. Our closer examination of the electrostatic grain shattering mechanism leads to a significant increase in its relative importance. Our results imply that the amount of dust destroyed by X-rays associated with GRBs may considerably exceed that destroyed by the prompt UV pulse alone.

Although there is a great degree of uncertainty regarding possible collimation and beaming of GRBs, our results are very nearly independent of these questions. Only the X-rays radiated along our line of sight and the dust grains lying along that same line of sight are relevant to the issues we pursue. So long as the photons in the optical/UV afterglow travel within the cone filled by the X-ray beam, it does not matter how large those solid angles are.

2. PHENOMENOLOGY OF X-RAY AND OPTICAL EMISSION ASSOCIATED WITH γ-RAY BURSTS

When considering destruction of dust, we are primarily concerned with the spectral window from the X-ray through the optical, where the cross section for photons to interact with dust grains is largest. Dust grains can absorb optical and ultraviolet photons through a variety of continuous opacity mechanisms; X-rays are primarily absorbed by K-shell ionization of medium-Z elements such as C, Si, O, etc. The X-rays with which we are primarily concerned are therefore those whose rest-frame energies lie in the band from 0.3 to $\simeq 10$ keV, a stretch defined by the C K-edge at the low-energy end and the Fe K-edge (plus a small energy margin; see below) at the high-energy end.

In the case of the long (1–100 s) duration bursts, the X-ray emission is now known to be broken into two parts: a short (1–100 s) pulse, largely coinciding with the γ-ray burst itself; and a longer, smooth decline, known as the afterglow. The short duration bursts (<1 s) have been inaccessible to *BeppoSAX*, and their afterglow properties, if any, are at present unknown.

During the burst proper, the X-ray flux in the 0.3–10 keV band is strong and hard, with an energy spectral index α (flux per unit energy $\propto \epsilon^{-\alpha}$ for photon energy ϵ) typically between -1 and 1 (Band et al. 1993; Frontera et al. 2000). During the peak of the burst, this hard spectrum can continue up to or above 100 keV before it breaks. However, as the burst progresses, the break drops to lower energies and the X-ray spectrum softens, leading to a temporary increase in the 0.3–10 keV band (Frontera et al. 2000). As the burst fades, a prolonged afterglow phase begins.

Although the physics which produces the rapid, variable γ-ray and X-ray burst is not particularly well understood, there is good evidence that the afterglow is produced by synchrotron emission from electrons accelerated in the external shock between GRB ejecta and an ambient medium as predicted by Paczyński & Rhoads (1993), Katz (1994), and Meszaros & Rees (1997). This class of model leads to a broken power-law spectrum whose break frequencies evolve as power laws in time (Sari, Piran, & Narayan 1998) and has been reasonably successful at describing the observations.

Most afterglows are well fitted by power-law slopes $p \approx 2.3$ for the injected electron energy spectrum in the expanding fireball's external shock. The highest energy spectral break in the afterglow spectrum is usually the cooling break. At frequencies above the cooling break, the temporal decay of afterglow emission goes as $t^{1/2-3p/4}$, while at lower frequencies, it follows a shallower decay of $t^{3/4-3p/4}$. For observed afterglows, the cooling break passes through the X-ray band very early (observed at $t \ll 1$ day), but its passage through the optical band can occur anywhere from $t \ll 1$ day to $t \sim 2$ days (Galama et al. 1999). This means that the X-ray afterglow often fades faster than the optical afterglow.

As we will show below, both the X-ray flux and fluence are important in dust destruction by GRBs. The peak X-ray flux occurs during the GRB itself, with characteristic values of $\sim 10^{-7}$ ergs cm^{-2} s^{-1} for bursts detected by *BeppoSAX*. The relative contributions of the afterglow and the GRB itself to the X-ray fluence are discussed by Frontera et al. (2000), who find that each contributes $\sim 10^{-6}$ ergs cm^{-2} to the X-ray fluence from *BeppoSAX* bursts, although in individual cases the ratio of burst to afterglow X-ray fluence has been anywhere from $\sim \frac{1}{3}$ to ~ 3. (Practically, the fluence during the burst is determined by direct integration of the observed light curve during the duration of measurable γ-ray emission, while the fluence of the afterglow is determined by fitting power-law light curves to the observed points on the afterglow light curve. This phenomenological division is relevant for our calculations whether the physical mechanisms responsible for X-ray emission during the GRB and the afterglow differ or not.) The X-ray emission during the GRB is generally consistent with the extrapolation of the X-ray afterglow to early time (Frontera et al. 2000). For typical afterglow decay rates, at least half the X-ray afterglow fluence is typically received within $10 \times \Delta t_{\rm GRB}$, where $\Delta t_{\rm GRB}$ is the duration of the GRB (see Dal Fiume et al. 2000 for further discussion of this point).

Given how rapidly even the afterglow X-ray flux decays, we conclude that any effects on intervening dust due to X-ray irradiation take place within a few minutes of the burst. Thus, any attempts to watch dust destruction in progress will require very fast response.

3. EFFECT OF X-RAYS ON DUST

3.1. *Elementary Interactions*

The fundamental interaction between X-rays and dust grains is K-shell photoionization of medium-Z elements such as O, Si, S, and Mg, and either K-shell or L-shell photoionization of Fe. When K-shell photoionization occurs, a fast electron is created with energy equal to the difference between the absorbed photon energy and the ionization threshold for the relevant shell. Very soon after, the atom relaxes by one of two processes: Auger ionization (which results in a second fast electron with energy slightly less than the initial ionization threshold) or fluorescence. For elements in this range of atomic number, Auger ionization usually dominates.

As these fast electrons travel through the grain, they lose energy by Coulomb scattering other electrons. In some cases the scattered electrons also begin travelling through the grain. However, no electron gets very far unless its initial energy is fairly high. According to Draine & Salpeter (1979), the range of a fast electron (energy 300 eV to 1 MeV) in typical interstellar dust materials is

$$R \simeq 0.03 \rho^{-0.85} E_{\rm keV}^{1.5} \ \mu{\rm m} \ , \qquad (1)$$

where ρ is the density in g cm^{-3} and $E_{\rm keV}$ is the initial electron energy in keV. Thus, in grains as large as ~ 0.1 μm,

only electrons either more energetic than several keV or produced very close to the grain surface can escape (see Dwek & Smith 1996 for a more detailed treatment of the effects of photoionization in dust grains). Below we will discuss a second mechanism that can also inhibit electron loss.

Electron Coulomb scattering also has another effect on the grain. Significant energy transfer to secondary electrons is likely to break chemical bonds, weakening the crystal structure. We will return to the consequences of this fact later.

3.2. *Heating and Sublimation*

The immediate result, however, of many X-ray photoionizations is simply the heating of an individual grain at a rate of

$$G \approx 3 \times 10^{-3} \frac{\mathscr{T}_h(x_K, \alpha, N)}{2+\alpha} \frac{E_{51}\,\sigma_{-19}\,n_{23}}{D_{100}^2} \frac{a_{0.1}^3}{t_{10}} x_K^{1-\alpha} \times [1-(1+x_{\min}/x_K)^{-(2+\alpha)}] \text{ ergs s}^{-1}, \quad (2)$$

where the grain is assumed to be optically thin to the X-rays, as is generally the case. Here E_{51} is the total energy radiated in X-rays in the sense of $4\pi\epsilon dE_\epsilon/d\Omega$, evaluated at $\epsilon_0 = 1$ keV and scaled to 10^{51} ergs, and $dE_\epsilon/d\Omega$ is the energy radiated per unit energy per solid angle. Other symbols are σ_{-19}, the K-shell edge cross section in units of 10^{-19} cm^2; n_{23}, the atomic density in the grain in units of 10^{23} cm^{-3}; x, photon energy in keV; $a_{0.1}$, the grain size in units of 0.1 μm; t_{10}, the characteristic time of the X-ray emission scaled to 10 s; D_{100}, the distance from the γ-ray burst source to the dust in units of 100 pc; α, the (energy) spectral index, defined in the sense that $E_\epsilon \propto \epsilon^{-\alpha}$; N, the H atom column density along the line of sight; x_K, the energy in keV of the most important K-edge in the grain; and $x_{\min}$, the minimum energy (in keV) of electrons able to escape from the grain (see more extensive discussion below). In deriving this equation, we have taken $\sigma \propto x^{-3}$ for $x > x_K$. In practice, as noted before, the low-energy X-ray spectrum of GRBs during the burst varies both between bursts and during individual bursts, with values ranging over the interval $-1 \lesssim \alpha \lesssim 1$ (Frontera et al. 2000). The factor $\mathscr{T}_h$ describes the transparency to X-rays of the ISM between the burst source and the dust grains, suitably averaged over the X-ray spectrum of the GRB. We will discuss this factor at greater length in § 4.1. (A glossary of symbols appears in Table 1.)

It will be convenient to group the combination of fiducial factors $\sigma_{-19}\,n_{23}\,E_{51}\,D_{100}^{-2}$; we call this quantity the modified fluence and symbolize it as A. The combination $\sigma_{-19}\,n_{23}$ should be order unity, its exact value depending on the grain composition. For example, if the grains are olivine, whose chemical composition is Mg_2SiO_4 (as found in O-rich environments: Waters et al. 1996), $\sigma_{-19}\,n_{23} \simeq 2$ for photons above the Si-edge at 1.9 keV. On the other hand, the value of $\sigma_{-19}\,n_{23}$ for graphite is $\simeq 17$, with the threshold $x_K = 0.28$.

Two processes, radiative cooling and sublimation, counterbalance heating. Following Spitzer (1978), we write the rate of radiation cooling per grain as $4\pi a^2 \times \pi \int Q_a B_\lambda\, d\lambda$, where Q_a is the absorption efficiency of the grain and B_λ is the Planck function. For grains smaller than $\simeq 1$ μm, Q_a can be considerably less than unity because the characteristic wavelength of their thermal radiation is rather larger than their size. In the small grain limit ($2\pi a \ll \lambda$), $Q_a \approx 8\pi a/\lambda \times \text{Im}[(m^2-1)/(m^2+2)]$, with m the complex index of refraction of the grain material and Im denoting the imaginary part. In the relevant temperature range (i.e., $T \sim 2000$ K), for most grain materials $\text{Im}[(m^2-1)/(m^2+2)]$ is almost independent of λ over the range of wavelengths that dominate the integral ($\lambda \sim ch/kT$). Rather than following the usual scaling ($\propto T^4$), the cooling rate is then $\propto T^5$. Typical values of $\text{Im}[(m^2-1)/(m^2+2)]$ are in the range 0.01–0.1; we adopt a fiducial value of 0.065 so that the cooling rate per grain becomes $3.1 \times 10^{-3} a_{0.1}^3\, T_3^5\, \phi$ ergs s^{-1}. With this choice, we can estimate values of the material-dependent correction factor ϕ by comparing to the cooling rate computed by Waxman & Draine (2000) for the temperature range 2000 K $\lesssim T \lesssim$ 3000 K based on the optical constants of Draine & Lee (1984): $\phi \approx 0.3$ for silicates, $\phi \approx 3$ for graphite, and $\phi \approx 1$ is a representative average value.

Following Waxman & Draine (2000) and Guhathakurta & Draine (1989), we write the sublimation rate as

$$\frac{da}{dt} = -n^{-1/3} \nu_0 \exp\left(-\frac{H}{kT}\right). \quad (3)$$

Here the characteristic frequency $\nu_0 \sim 10^{15}$ s^{-1} and binding energy per atom $H \sim 10^{-11}$ ergs depend on the grain material. Estimates for graphite are $\nu_0 \approx 2 \times 10^{14}$ s^{-1} and $H \approx 1.1 \times 10^{-11}$ ergs, while for silicates, represented by Mg_2SiO_4, $\nu_0 \approx 2 \times 10^{15}$ s^{-1} and $H \approx 0.94 \times 10^{-11}$ ergs (Waxman & Draine 2000; Guhathakurta & Draine 1989). For the purpose of these estimates (and in the absence of published values for H and ν_0 pertaining to carbon-rich grains with other structures), we will suppose that the graphite numbers apply to all carbonaceous grains. Clearly, the sublimation rate is very sensitive to the temperature.

Neglecting fluctuations due to absorption of individual energetic photons (these will be most important in very small grains, of course), the grain temperature is determined by the heat balance equation

$$\frac{d\mathscr{Q}}{dt} = 3 \times 10^{-3} \frac{\mathscr{T}_h A}{(2+\alpha)t_{10}} a_{0.1}^3\, x_K^{1-\alpha} \times [1-(1+x_{\min}/x_K)^{-(2+\alpha)}] - 3.1 \times 10^{-3} a_{0.1}^3\, T_3^5\, \phi - 2.7 \times 10^{10} a_{0.1}^2\, n_{23}^{2/3}\, \nu_{15}\, H_{-11} \times \exp(-72.5 H_{-11}/T_3) \text{ ergs s}^{-1}, \quad (4)$$

where the three terms on the right-hand side correspond to X-ray heating, radiative cooling, and sublimation cooling. Here $\mathscr{Q}$ is the total thermal energy in the grain, T_3 is temperature in units of 10^3 K, ν_{15} is the characteristic frequency ν_0 in units of 10^{15} Hz, and H_{-11} is the binding energy per atom in units of 10^{-11} ergs. The sublimation cooling (following Waxman & Draine 2000) is simply H for each atom removed from the grain.

As shown by equation (4), radiation and sublimation compete to control the temperature. Although both increase rapidly with increasing temperature, sublimation has by far the more sensitive dependence on temperature in this regime. Consequently, radiation dominates at low temperatures, sublimation at high. Following Waxman & Draine (2000), we find the temperature that divides these

TABLE 1

GLOSSARY OF SYMBOLS

Symbol	Definition	Section
A	Modified fluence: $\sigma_{-19} n_{23} E_{51} D_{100}^{-2}$	3.2
$a_{0.1}$	Grain size (in units of 0.1 μm)	3.2
$B_\lambda(T)$	Planck blackbody radiation function	3.2
C	Modified radiated X-ray energy: $= D_{100}^2 A$	4.2
D_{100}	Distance from burst to dust (in units of 100 pc)	3.2
E_ϵ	Energy density of radiated X-rays (in units of ergs keV^{-1})	3.2
E_{51}	Fiducial energy radiated in X-rays: $4\pi\epsilon dE_\epsilon/d\Omega$ evaluated at $\epsilon = 1$ keV (in units of 10^{51} ergs)	3.2
e	Electron charge, with a sign convention that $e = -\|e\|$	3.3
G	Rate of heating of a grain (in units of ergs s^{-1})	3.2
H_{-11}	Binding energy per atom in a grain (in units of 10^{-11} ergs)	3.2
k_b	Boltzmann constant	3.2
N	H atom column density along the line of sight	3.2
n_{23}	Atomic density in a grain (in units of 10^{23} cm^{-3})	3.2
p	Power-law index of the burst injected electron energy spectrum	2
$\mathcal{Q}$	Total thermal energy in the grain (in units of in ergs)	3.2
Q_a	Optical absorption efficiency of a spherical grain	3.2
$\langle Q_A \rangle_T$	Absorption efficiency Q_a averaged over a Planck spectrum of temperature T	3.2
$R_{\rm ion}$	Ionization rate of a grain (in units of electrons per second)	3.3
S_{10}	Stress across a grain (in units of 10^{10} dyne cm^{-2}	3.3
$S_{\rm crit}$	Stress sufficient to shatter a grain	4.3
$S_{\rm crit,10}$	$S_{\rm crit}$ (in units of 10^{10} dyne cm^{-2})	4.3
T_3	Temperature (in units of 10^3 K)	3.2
T_{e4}	Electron temperature (in units of 10^4 K)	3.3
$T_{\rm eq}$	Equilibrium temperature of a grain	3.2
$T_{r=s}$	Temperature where radiation cooling equals sublimation cooling	3.2
$T_{\rm sub}$	Temperature required to sublimate a grain during the burst	3.2
$\mathcal{T}_h$	Flux-weighted transparency to X-rays of the ISM	3.2
$\mathcal{T}_i$	Photon-number weighted transparency to X-rays of the ISM	3.3
t_{10}	Characteristic time of the X-ray emission scaled to 10 s	3.2
x	Photon energy (in units of keV)	3.2
x_c	Energy above which the ISM is effectively transparent to X-rays	3.3
x_K	Energy in keV of the most important K-edge in the grain	3.2
$x_{\rm min}$	Minimum energy (in units of in keV) of electrons able to escape from grain	3.2
Z	Atomic number	2
Z_g	Grain charge in units of electron charge	3.3
α	Energy spectral index of the burst X-ray flux	2
ϵ	Photon energy	2
ϕ	Correction factor of order unity used in radiative cooling equations	3.2
ρ	Density of a grain (in units of g cm^{-3})	3.1
σ_{-19}	K-shell edge cross section (in units of 10^{-19} cm^2)	3.2

NOTE.—Some symbols used in a single equation or paragraph and those used only in the Appendix have been excluded.

two regimes by solving the equation

$$T_{r=s} = 2980 H_{-11} \times \left\{1 - 0.041 \ln\left[\frac{a_{0.1}\,\phi}{n_{23}^{2/3} v_{15} H_{-11}} \left(\frac{T_{r=s}}{2980\ \mathrm{K}}\right)^5\right]\right\}^{-1} \mathrm{K}\ . \quad (5)$$

Note that we have introduced scaling factors into the logarithm so that when the parameters all attain their fiducial values, $T_{r=s} = 2980$ K. Because the typical $T_{r=s}$ is so high, for most of the volume of interest radiation cooling dominates, as the burst is unable to heat the dust to $T_{r=s}$. The equilibrium temperature is then

$$T_{\rm eq} = 1000 \left[\frac{A \mathcal{T}_h x_K^{1-\alpha}}{(2+\alpha)\phi t_{10}}\right]^{1/5} \mathrm{K}\ . \quad (6)$$

We have dropped the correction factor involving $x_{\rm min}$ from this expression because, except in the case of the very smallest grains, it does not substantially alter the result.

When $|da/dt| > a/t$ for grain size a and X-ray emission duration t, the grain is effectively destroyed by sublimation during the burst and its aftermath. If we approximate the X-ray light curve by a square wave with this duration, the criterion for whether a grain is completely sublimated is equivalent to a condition on its equilibrium temperature:

$$T_{\rm eq} \geq T_{\rm sub} = \frac{2360 H_{-11}}{1 - 0.033 \ln(a_{0.1} n_{23}^{1/3} v_{15}^{-1} t_{10}^{-1})}\ \mathrm{K}\ , \quad (7)$$

where $T_{\rm sub}$ is, of course, the temperature required to sublimate the dust grain during the burst. The critical temperature for sublimation is most sensitive to the binding energy per atom H, but also depends on grain size, density, and characteristic sublimation rate ν_0. Comparing the result of equation (7) to equation (6), we see that the flux ($\propto A/t_{10}$) must be rather greater than our fiducial value in order to completely sublimate most grains.

Comparing the expressions for $T_{r=s}$ and $T_{\rm sub}$, we also see that in most cases the sublimation temperature is reached

while cooling is still radiation dominated. Sublimation cooling dominates radiative cooling at temperatures below $T_{\rm sub}$ only when

$$t_{10} \leq 1.7 \times 10^{-3} \phi^{-1} n_{23}^{-1/3} H_{-11} \left(\frac{T_{\rm sub}}{2980}\right)^{-5} . \quad (8)$$

Sublimation cooling is therefore relevant only when the burst is very short: $\lesssim 0.02$ s. This time is coincidentally comparable to the thermal equilibration timescale for a grain at these temperatures ($\sim 10^{-3}$ s). Thus, we do not examine closely the case where the equilibrium grain temperature is set primarily by sublimation cooling because any grain so close to the burst that this regime applies will be destroyed well before the burst ends.

We have so far neglected grain temperature fluctuations, which can matter because the sublimation rate is such a strong function of grain temperature. Such fluctuations may arise both from the rapid substructure that characterizes most GRB light curves and from the discrete nature of the X-ray heating. All grains will be affected by the light curve variations, while only grains with $a \lesssim 0.01$ μm will be substantially affected by the second mechanism. To account for such variations fully, one could calculate the temperature history of a particular grain for a particular burst using equation (4) and so determine the total grain erosion $\int da/dt(T)dt$. Such a treatment is beyond the scope of this paper. We simply note that for a typical burst, the fluctuations in heating rate will result in more grain erosion than a uniform flux $\propto A/t_{10}$ would naively produce.

Thus, for typical burst parameters, we find that the conditions under which X-ray heating can vaporize both carbon-rich and silicate grains are fairly similar. In both cases, fluxes somewhat greater than those associated with our fiducial parameter values are required. Coatings of more volatile materials (ices, etc.) can, of course, be removed much more readily.

Waxman & Draine (2000) pointed out that the optical/UV afterglow can also heat the grains strongly enough to evaporate them. Although the peak flux in X-rays is often greater than in the optical/UV, grains absorb a larger fraction of the optical/UV light striking them than of the X-rays. Consequently, which band is the more effective in sublimating grains depends on details. We contrast the two mechanisms in Figure 1 (see the discussion at the end of § 3.3).

3.3. *Charging and Electrostatic Shattering*

Although an electron that escapes does not contribute to grain heating, it nonetheless can have a deleterious effect on the dust it leaves behind. As the freed charge exits the grain, it leaves a positive charge, and even if the X-ray flux in the burst proper is too weak to evaporate grains along the line of sight, the buildup of electrostatic stress (Waxman & Draine 2000) from these liberated electrons can pose a lethal peril to the grains.

The rate of charging is simply the rate of photoionizations by photons of high enough energy that the primary ionized electron has a range greater than the size of the grain. The majority of K-shell photoionization events in medium-Z elements lead to an immediate second ionization by the Auger mechanism, but we make the conservative approximation that the energies of the Auger electrons are all below the threshold for escape. Assuming that all individual grains are optically thin to X-ray photons, this rate is

$$R_{\rm ion} \simeq 2.2 \times 10^{6} \frac{A \mathscr{T}_i(x_{\rm min}, \alpha, N)}{3+\alpha} \frac{a_{0.1}^3}{t_{10}} x_K^{-\alpha} \times \left(\frac{1+x_{\rm min}}{x_K}\right)^{-(3+\alpha)} {\rm s}^{-1} . \quad (9)$$

The function $\mathscr{T}_i$ is almost like $\mathscr{T}_h$. The only difference is that the rate of charging is proportional to the *number* of absorbed photons, whereas the rate of heating is proportional to the *energy* of absorbed photons, so the transparency factor $\mathscr{T}_i$ is weighted according to photon number rather than energy. We defer further discussion of both factors to § 4.1.

We emphasize that heating and charging depend on the X-ray irradiation in different ways. The grain temperature depends on the X-ray *flux*, but the ultimate grain charge depends on the X-ray *photon fluence*. That is, because each sufficiently energetic photon removes one electron, what matters is the total number of photons in the energy range that, when absorbed in a grain, expel an electron. This energy range is quite restricted. The low-energy end is fixed by the lowest K-edge plus $x_{\rm min}$, and as the absorption cross section drops rapidly with energy above threshold, the high-energy end is roughly twice the highest energy K-edge plus $x_{\rm min}$. Consequently, grain sublimation depends on the peak X-ray flux, whereas grain charging depends on the integrated number of photons in the appropriate energy range.

Two different mechanisms can control $x_{\rm min}$: energy loss in the grain and restraint by the same electrostatic potential that is built up by charging. Energy loss in the grain poses a threshold $x_{\rm min} \simeq 4a_{0.1}^{2/3}$ for a grain with density $\simeq 3$ g cm^{-3}. This threshold for escape is great enough that in most cases, charging is little affected by intervening absorption. This is because there is a critical energy x_c above which the ISM is effectively transparent, and typically $x_{\rm min} + x_K > x_c$ (further discussion of this point can be found in § 4.1). On the other hand, the electrostatic binding energy of an electron at the grain surface is

$$-eV = \frac{Z_g e^2}{a} = 1.4 \left(\frac{Z_g}{10^5}\right) a_{0.1}^{-1} \ {\rm keV} , \quad (10)$$

where Z_g is the grain charge in electron units and e is the electron charge (with a sign convention that $e = -|e|$). The magnitude of the potential becomes larger than the local loss threshold when

$$Z_g > 3 \times 10^5 a_{0.1}^{5/3} . \quad (11)$$

Unless the dust is in an environment with extremely high electron density, recombination with ambient electrons is far too slow to compete with burst photoionization. Allowing for the attractive focussing due to the grain potential, the electron-grain cross section is

$$\sigma_{gr,e} = \sigma_{\rm geom} \left(1 - \frac{2eV}{3kT_e}\right) , \quad (12)$$

where $\sigma_{\rm geom}$ is the ordinary geometric cross section of the grain and T_e is the electron temperature. When the grain potential is large enough to create an interesting stress, $|eV| \gg kT_e$ unless the ambient electrons are extremely hot.

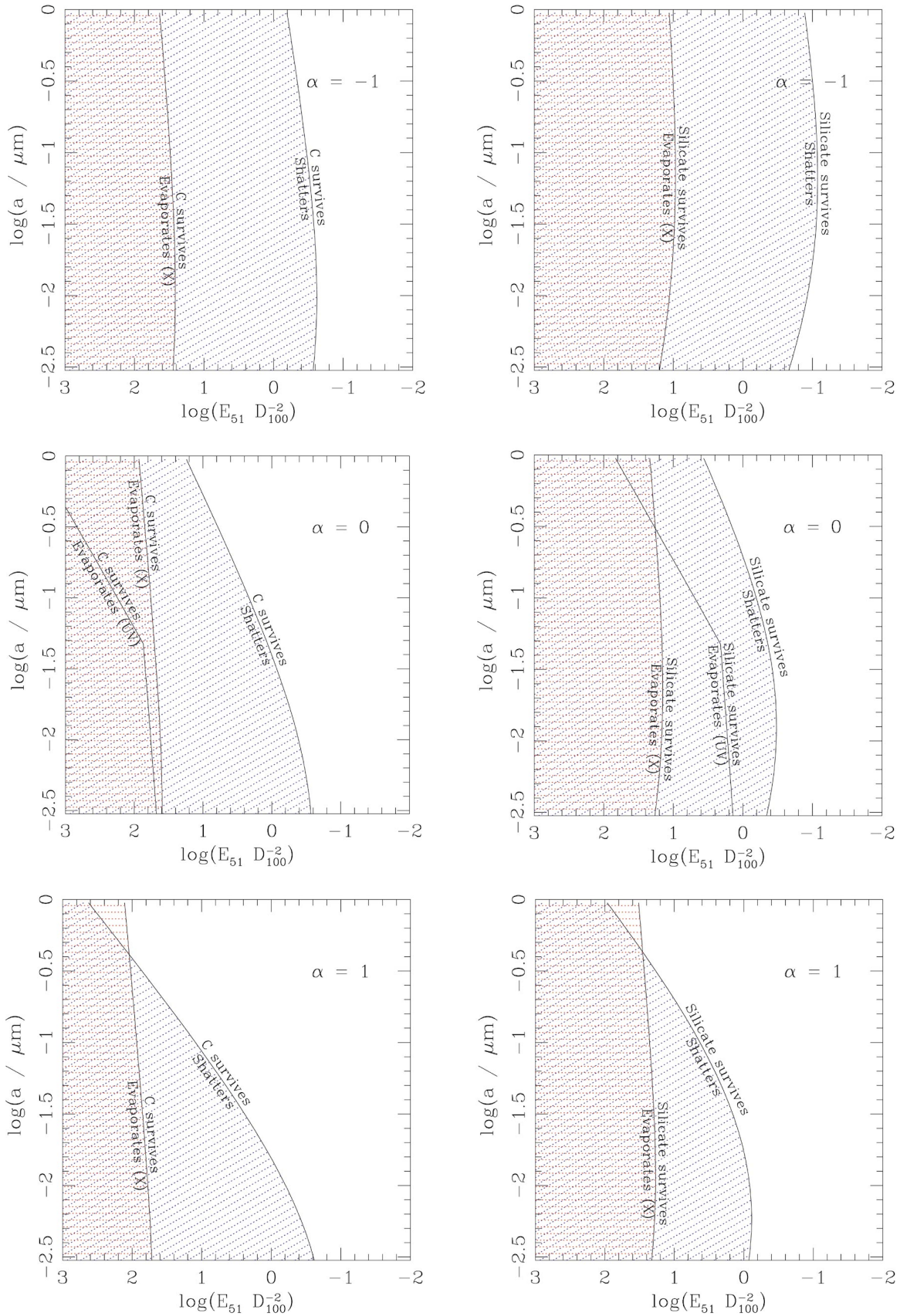

FIG. 1.—Grain destruction thresholds as a function of scaled GRB fluence $E_{51}\,D_{100}^{-2}\,\mathcal{F}$ and grain radius a. The six panels correspond to the X-ray spectral indices $\alpha = -1$, 0, and 1 for carbonaceous grains (*left side*) and silicate grains (*right side*). Other relevant parameters were taken at their fiducial values ($S_{10} = 1$, $t_{10} = 1$, ϕ as given by Draine & Lee [1984] for the respective grain compositions); changes to these would affect the relative importance of the different destruction mechanisms considered (see equations). All panels show thresholds for (1) grain shattering by electrostatic stress and (2) grain evaporation by X-ray heating. In the $\alpha = 0$ case, we also show the threshold for (3) grain evaporation by UV and optical heating.

Taking $\sigma_{\rm geom} = \pi a^2$, we find that the recombination rate is

$$R_{rec} \simeq 23 n_e a_{0.1} T_{e4}^{-1/2} \left(\frac{Z_g}{10^5}\right) \ {\rm s}^{-1} \tag{13}$$

for electron density n_e. Comparing this rate to the rate estimated in equation (9), we see that electron recombination is unlikely to be important. Although the UV pulse associated with the burst itself might transform a dense neutral region into a plasma with a high enough electron density for recombination to be competitive, this can only occur much closer to the burst than the critical distance for grain destruction by evaporative heating.

Neither of the mechanisms controlling the energy threshold depends strongly on the grain composition (only the density matters, and all the different plausible compositions have similar density). Consequently, $R_{\rm ion}$ increases roughly in proportion to $(A\mathscr{T}_i)x_K^3$. The positive dependence on x_K is due to the greater cross section when the photon energy is closer to the threshold. Although σ_K is somewhat greater for lower Z elements, it does not change enough with Z to outweigh the proportionality of $R_{\rm ion}$ to x_K^3. Consequently, higher Z compositions (e.g., silicates) are ionized more rapidly than carbonaceous grains. The contrast is about a factor of 10 in the quantity $\sigma_{-19} n_{23} x_K^3$, from about 0.37 for pure C to $\simeq 3.4$ for silicates.

The electric stress S created by this potential depends on the shape of the grain, as well as on the mobility of charges within the grain. For example, in a perfectly conducting grain all the charge would migrate to the outside. If the grain were spherical, the physical stress would be symmetrically distributed around the grain. However, sharp corners on a good conductor will be loci of particularly large stress. Insulating materials would be likely to have more uniformly distributed stress, for the charge density should simply be proportional to the initial K-shell electron density. Unfortunately, our knowledge of the detailed shape and electrical properties of grains is very shaky, and it is quite likely that grains exist across a wide range of shapes and conductivity (see, e.g., Mathis 1998 for a discussion of the issues involved). Despite these uncertainties, we can at least make an order of magnitude estimate of the stress:

$$S \equiv \frac{E^2}{4\pi} \sim \frac{(Z_g e)^2}{4\pi a^4} = 1.8 \times 10^{10} \left(\frac{Z_g}{10^5}\right)^2 a_{0.1}^{-4} \ {\rm dyne \ cm}^{-2} \ . \tag{14}$$

To put this in context, it is necessary to estimate the tensile strength of interstellar grains. Much uncertainty also attaches to this number. Grains with unflawed crystal structure could have tensile strengths $S_{\rm crit}$ as high as 10^{11} dyne cm^{-2} (Draine & Salpeter 1979). On the other hand, impurities, lattice dislocations, and other imperfections could greatly reduce the tensile strength. Some (e.g., Burke & Silk 1974) have suggested a value as low as $\sim 10^9$ dyne cm^{-2}. If grains are highly porous structures (as suggested by Mathis 1996), the critical stress might be still smaller. For the current problem, the large flux of energetic photons bombarding the grain is likely to damage the grain's crystalline structure heavily during the course of the burst. Thus, the highest estimates of the breaking stress are probably unrealistic in this context. In the following estimates, we will write the critical stress as $S_{\rm crit,10} \equiv S_{\rm crit}/10^{10}$ dyne cm^{-2}.

For most grain compositions and for larger grains, $x_{\rm min} > x_K$ because, with the exception of Fe, all the elements commonly found in grains have $x_K < 2$, whereas $x_{\rm min} \simeq 4a_{0.1}^{2/3}$. With that assumption, we find that when internal energy loss is the limiting factor, the final charge of a grain is

$$Z_g \simeq \begin{cases} 1.1 \times 10^5 A\mathscr{T}_i a_{0.1}^{1-2\alpha/3} \left(\dfrac{3}{3+\alpha}\right) 4^{-\alpha} x_K^3 & \text{(general } \alpha\text{)} \\ 1.1 \times 10^5 A\mathscr{T}_i a_{0.1} x_K^3 & \alpha = 0 \\ 1.9 \times 10^4 A\mathscr{T}_i a_{0.1}^{1/3} x_K^3 & \alpha = 1 \ , \end{cases} \tag{15}$$

resulting in a final stress

$$S \simeq \begin{cases} 2.1 \times 10^{10} (A\mathscr{T}_i)^2 a_{0.1}^{-2-4\alpha/3} \left(\dfrac{3}{3+\alpha}\right)^2 4^{-2\alpha} x_K^6 & \text{(general } \alpha\text{)} \\ 2.1 \times 10^{10} (A\mathscr{T}_i)^2 a_{0.1}^{-2} x_K^6 & \alpha = 0 \\ 6.9 \times 10^8 (A\mathscr{T}_i)^2 a_{0.1}^{-10/3} x_K^6 & \alpha = 1 \ {\rm dyne \ cm}^{-2} \ . \end{cases} \tag{16}$$

The above equations apply so long as local losses dominate the energy requirement for electrons to escape the grain. On the other hand, if the grain charge becomes sufficiently large, the energy required to escape the grain's electrostatic potential exceeds the local losses. Combining earlier results, we find that the potential dominates if

$$A\mathscr{T}_i \geq 2.8 a_{0.1}^{2(1+\alpha)/3} \left(\frac{3+\alpha}{3}\right) 4^{\alpha} x_K^{-3} \ . \tag{17}$$

Equation (17) may be interpreted to mean that when the fluence accumulated by a grain exceeds a minimum value, it enters the potential-limited charging regime. However, it is also possible that by that time it has already accumulated a charge so great that it has been shattered. For the criterion of equation (17) to be met, and yet for the grain not to have been already destroyed, the stress given by equation (16) must be less than the critical stress. Combining these two criteria, we find that grains survive into the potential-limited regime only if the critical breaking stress

$$S_{\rm crit} > 2 \times 10^{11} a_{0.1}^{-2/3} \ {\rm dyne \ cm}^{-2} \ . \tag{18}$$

On this basis, we conclude that the potential-limited regime is reached by only the biggest and strongest grains.

When charging is limited by the electrostatic potential, the eventual charge of the grain is

$$Z_g \simeq \begin{cases} \left[8 \times 10^{21} (1.4 \times 10^{-5})^{-\alpha} \left(\dfrac{\alpha+4}{\alpha+3}\right) A\mathscr{T}_i a_{0.1}^{\alpha+6} x_K^3 \right]^{1/(4+\alpha)} & \text{(general } \alpha\text{)} \\ 3.2 \times 10^5 (A\mathscr{T}_i)^{1/4} a_{0.1}^{3/2} x_K^{3/4} & \alpha = 0 \\ 2.3 \times 10^5 (A\mathscr{T}_i)^{1/5} a_{0.1}^{7/5} x_K^{3/5} & \alpha = 1. \end{cases} \tag{19}$$

Thus, when the grain charge is limited by the electrostatic potential itself, it depends far more on grain size than on the

strength of the burst. In this regime, the final stress is

$$S \simeq \begin{cases} 1.9 \times 10^{11} q_1(\alpha)(A\mathscr{T}_i)^{2/(\alpha+4)} a_{0.1}^{-(4+2\alpha)/(4+\alpha)} x_K^{6/(\alpha+4)} \\ \qquad\qquad \text{(general } \alpha\text{)} \\ 1.9 \times 10^{11} (A\mathscr{T}_i)^{1/2} a_{0.1}^{-1} x_K^{3/2} \\ \qquad\qquad \alpha = 0 \\ 1.0 \times 10^{11} (A\mathscr{T}_i)^{2/5} a_{0.1}^{-6/5} x_K^{6/5} \\ \qquad\qquad \alpha = 1 \text{ dyne cm}^{-2} . \end{cases} \tag{20}$$

Here $q_1(\alpha) = [0.24^{\alpha}(3/4)^{(\alpha+4)/4}(\alpha+4)/(\alpha+3)]^{2/(\alpha+4)}$ is a slowly varying function of α with value $q_1(0) = 1$.

We conclude that if $A > 1$, the stress should be great enough to break any but the strongest and largest grains; most grains should crack quite quickly. Note that in all cases for which $x_{\min} > x_K$, whether the charging threshold is set by local losses or by the grain potential, and for any reasonable X-ray spectral slope, a shorter time is required to charge smaller grains to a given stress. A detailed discussion of the (relatively small) additional fluence required to break grains down to very small sizes may be found in the Appendix.

Waxman & Draine (2000) also discussed this mechanism of grain destruction, but made several simplifying assumptions. They supposed that there was a uniform photoionization threshold of 10 keV and estimated the average photoionization cross section per electron at 10^{-24} cm^2. As a result, our estimate of the grain destruction rate by this mechanism is rather higher than theirs.

We summarize all these results in Figure 1. This figure shows the fluence $E_{51} D_{100}^{-2}$ required to either evaporate or shatter grains of size a and zero charge (i.e., in the notation of the Appendix, the fluence corresponding to $t_{\rm break}^0$). The spans in fluence and grain size are chosen so as to display the widest plausible range in these parameters while maintaining the validity of our physical assumptions. For example, grains smaller than $\simeq 30$ Å $= 0.003$ μm behave more like large molecules than grains; on the other hand, grains larger than 1 μm can be optically thick to some photoionizing X-rays and are no longer in the dipole limit when radiating infrared photons. To specify the curve positions, we set all scaling factors to unity, i.e., $\mathscr{T}_h = \mathscr{T}_i = 1$, $x_K = 1$, $S_{\rm crit,10} = 1$, $t_{10} = 1$, and $T_{\rm sub} = 2300$ K. The plotted curves account for the inefficiency of X-ray heating in small grains due to the relatively easy escape of fast electrons (eq. [1]). They also use the full forms of equations (2) and (9); i.e., they do not make the approximation that $x_{\min} \gg x_K$. The comparison between X-ray and optical/UV effects is fixed by using the observed fluxes of GRB 990123 (Akerlof et al. 1999; Williams et al. 1999; E. Costa 2000, private communication). This burst was the fiducial burst chosen by Waxman & Draine (2000). Because the X-ray spectrum of GRB 990123 is not yet available, we have assumed a spectral index of $\alpha = 0$, which is perhaps the most typical value for the bursts in the *BeppoSAX* sample (Frontera et al. 2000). The UV evaporation rate is calculated as in Waxman & Draine (2000), but with the modification that the absorption efficiency $Q_{\rm UV} \equiv \min(1, 2\pi a/\lambda_*)$ in order to allow for the reduction in efficiency that occurs when grains are smaller than the wavelength. For the purpose of the figure, we choose a characteristic wavelength $\lambda_* = 3000$ Å.

As the figure makes plain, many γ-ray bursts can eliminate large parts of the dust-grain population. For almost all reasonable parameters, the electrostatic mechanism is a more powerful destroyer of grains than is evaporation, whether due to X-rays or UV. Silicate grains are somewhat more sensitive to shattering than carbon-rich grains because the cross section for X-rays energetic enough to expel electrons is larger (the contrast is greatest for relatively large grains). On the other hand, evaporation acts more powerfully on carbonaceous grains because they are able to absorb softer photons than silicate grains can.

The grain-size dependence of the critical fluence for shattering is more complicated to describe (the approximate scalings mentioned in this paragraph are derived in the Appendix). When $x_{\min} \gg x_K$ is a good approximation, the critical fluence declines with decreasing a, roughly $\propto a^{1+2\alpha/3}$. This approximation is best for large grains; the dividing line between "large" and "small" for this purpose falls at smaller a for carbon-rich grains than for silicates. On the other hand, when $x_{\min}$ is not much larger than x_K, the critical fluence grows with decreasing a, roughly $\propto a^{-1}$. Thus, particularly when exposed to soft X-ray spectra, small carbon-rich grains are more readily destroyed than large ones. The same trend applies to silicate grains, but more of parameter space is occupied by "small" grains for which $x_{\min}$ is not large compared to x_K; "small" silicate grains may require as much or more fluence to break as "large" ones, particularly when the X-ray spectrum is very hard. The critical flux for X-ray evaporation is relatively insensitive to grain size because both heating and cooling rates scale approximately $\propto a^3$.

For all three values of α, the critical fluence dividing the potential-limited grain-charging regime from the local loss-limited regime is significantly greater than the critical fluence for shattering grains. This fact means that, at least when our fiducial parameters are appropriate (most importantly, for $S_{\rm crit,10} = 1$), grains shatter before their charge becomes so great that the potential becomes important.

If electrostatic stresses are, for some reason, ineffective, evaporation can also destroy grains, but for a smaller range of parameters. If the optical/UV–to–X-ray flux ratio of GRB 990123 is representative of most bursts, UV heating is generally the more important effect for small grains, X-ray heating for large (although the dividing line depends on grain composition). The primary reason for this is that the absorptive efficiency of dust grains is fairly high in the optical/UV band, but falls rapidly with increasing energy through the X-ray band. All but the thickest dust grains are optically thin throughout almost the entire relevant range of X-ray energies.

4. GRAIN DESTRUCTION DISTANCES

In the simplest circumstances the maximum distance from the burster at which each mechanism will be effective may be read off the curves in the figure. In this section we provide further guidance on estimation of these maximum distances: we discuss how those curves may change due to intervening absorption, and we present some analytic approximations to estimate the critical destruction distances.

4.1. *Intervening Absorption*

Medium-Z atoms in the ISM of the host galaxy between the burst source and the dust may intercept X-rays before they strike the grains. Whether these atoms are able to do so depends on whether or not they are fully stripped of

electrons; the specific ionization stage of the atoms affects the magnitude of their photoelectric opacity to only a modest degree.

In the energy range between 538 eV (its edge when neutral) and 7.1 keV (the neutral Fe K-edge), O provides the single greatest contribution to X-ray photoionization opacity, so we concentrate on estimating the circumstances in which it may be fully ionized. As its ionization stage rises from neutral to H-like, the K-edge of O rises from 538 to 871 eV, with most of the change occurring between the Li-like and H-like stages. The cross section just above threshold varies relatively little, dropping from $\simeq 5 \times 10^{-19}$ cm^2 for O I to $\simeq 1.4 \times 10^{-19}$ cm^2 for O VIII (Verner & Yakovlev 1995). For each K-shell ionization in O I through O V, there is (on average) almost one Auger ionization. Therefore, in order for O to be fully stripped by the burst, a number fluence of photons above 500–800 eV $\gtrsim 2 \times 10^{19}$ cm^{-2} must pass through the region where the O is located. Scaled in terms of our fiducial parameters, the photon fluence above energy x_K in a burst is $5 \times 10^{17} x_K^{-\alpha} E_{51} D_{100}^{-2}$ cm^{-2}. Thus, we expect that closer than ~ 6 pc, a typical burst releases enough X-ray photons to strip all the O atoms; farther away, the O may be partially, but not completely, ionized. Recombination takes place so much more slowly (on a timescale of $\sim 10^{11} n_e^{-1}$ s) that it is irrelevant to burst afterglows.

If the ISM has solar abundances and the bulk of the absorbing column is located far enough from the burst that O (and similar atoms) are not fully ionized, the soft X-ray opacity for photons of energy $0.5 \lesssim x \lesssim 5$ scales roughly $\propto x^{-3+\delta}$, where $\delta \simeq 0.4$–0.6 depends on the ionization state (Morrison & McCammon 1983; Krolik & Kallman 1984). The departure from x^{-3} scaling is due to the summation of photoelectric opacity from many different elements, each having a different threshold energy (in contrast to the situation for dust, in which a few elements dominate the opacity of any particular grain). As a result there is effectively an energy x_c below which the ISM is optically thick, but above which it is transparent. The transparency factors $\mathscr{T}_i$ and $\mathscr{T}_h$ can then be evaluated by appropriate integrations:

$$\mathscr{T}_h \simeq \begin{cases} 1 & x_c < x_K \\ (x_K/x_c)^{2+\alpha-\delta} & x_K < x_c < x_K + x_{\min} \\ 0 & x_c > x_K + x_{\min} \end{cases} \quad (21)$$

and

$$\mathscr{T}_i = \begin{cases} 1 & x_c < x_K + x_{\min} \\ [(x_{\min} + x_K)/x_c]^{3+\alpha-\delta} & x_c > x_K + x_{\min} . \end{cases} \quad (22)$$

In effect, when $x_c > x_K$, x_c replaces x_K in the heating rate; similarly, when $x_c > x_K + x_{\min}$, x_c replaces $x_K + x_{\min}$ in the ionization rate.

In the ISM of an ordinary galaxy, typical total column densities are $N \sim 10^{21}$ cm^{-2}; however, compact star-forming regions may have column densities as much as 100 times greater. If the gas is nearly neutral, random lines of sight might have $x_c \simeq 0.55$ while lines of sight passing through giant molecular clouds or star-forming regions might have x_c as large as $\simeq 3.4$.

Because lower energy K-shell ionizing photons contribute primarily to heating, whereas higher energy photons (those above $x_K + x_{\min}$) contribute to ionization, intervening absorption can more easily affect heating than charging. Its effect can be particularly great on carbon-rich grains, whose x_K is much lower than in silicate grains.

However, as the figure demonstrates, we find that grain charging is the dominant grain destruction mechanism under almost all circumstances. Because $x_{\min}$ is usually at least a few keV (except for very small grains), soft X-ray absorption is most likely to affect the charging rate only for small, C-rich grains unless the absorbing column is relatively great. Even in those instances in which the column is larger than average, it is possible that most of the intervening matter is associated with a molecular cloud close enough to the burst that its C, N, O, etc., are fully ionized by the burst itself.

In the discussion so far we have not made any distinction between medium-Z atoms in grains or in the gas phase. This is because their K-shell opacity does not depend at all on the phase in which they are located. Consequently, unlike the situation regarding UV propagation, dust destruction is irrelevant to the soft X-ray opacity.

4.2. *X-Ray Heating*

We now estimate the destruction distance due to X-ray heating. The maximum distance for dust evaporation by this mechanism follows easily from equations (6) and (7). The condition for grain evaporation is

$$D_{100} \le 0.11 \times \left\{ \frac{C \mathscr{T}_h x_k^{1-\alpha}}{(2+\alpha)\phi t_{10} H_{-11}^5} \left(1 - 0.0326 \ln \left[\frac{a_{0.1} n_{23}^{1/3}}{v_{15} t_{10}} \right] \right)^5 \right\}^{1/2} , \quad (23)$$

where $C = E_{51} \sigma_{-19} n_{23} = D_{100}^2 A$. So long as the logarithm on the right-hand side is small, this expression is well approximated by

$$D_{100} \lesssim 0.11 \left[\frac{C \mathscr{T}_h x_k^{1-\alpha}}{(2+\alpha)\phi t_{10} H_{-11}^5} \right]^{1/2} \left(\frac{a_{0.1} n_{23}^{1/3}}{v_{15} t_{10}} \right)^{-0.0815} . \quad (24)$$

Two effects not contained in these equations will alter the grain destruction distance for small grains in opposite ways. First, as already remarked, small grains are heated less efficiently than large ones because it is easier for electrons to carry off the deposited energy. Second, we have used the equilibrium temperature. Thermal fluctuations due to the discreteness of the impinging X-ray photons can be substantial for very small grains, and may allow sublimation of these grains even when their equilibrium temperature is appreciably below $T_{\rm sub}$. The characteristic values of E_{51} should range from ~ 1 to ~ 10 based on *BeppoSAX* observations of GRBs 970228, 970508, and 971214 (Frontera et al. 2000), while t_{10} ranged from ~ 3 to ~ 5 for these same bursts. Thus, destruction distances in the range of 5–20 pc are reasonable for this mechanism.

4.3. *Grain Charging*

For grain shattering through charging, the destruction distance can be calculated separately for the cases where the energy requirement for an electron to escape the grain is dominated by internal energy losses or by electrostatic potential. The appropriate destruction distance will be the smaller of the two. Here we present several analytic approximations for the destruction distance, all valid for the regime in which $x_{\min} \gg x_K$. For the case of internal energy

losses, we find

$$D_{100} \leq 1.2\left(\frac{3}{3+\alpha}\right)^{1/2} 4^{-\alpha/2}\sqrt{C\mathscr{T}_i}\, S_{\rm crit,10}^{-1/4}\, a_{0.1}^{-1/2-\alpha/3} x_K^{3/2} . \quad (25)$$

For the case where electrostatic potential determines the minimum photon energy for charging, we instead find

$$D_{100} \leq 19 q_2(\alpha)\sqrt{C\mathscr{T}_i}\, S_{\rm crit,10}^{-1-\alpha/4} a_{0.1}^{-1-\alpha/2} x_K^{3/2} , \quad (26)$$

where $q_2(\alpha) = 1.02^{\alpha}[(3/4)^{1+\alpha/4}(\alpha+4)/(\alpha+3)]^{1/2}$. Thus, this mechanism can yield destruction distances considerably beyond those offered by evaporation; as the figures show, the contrast can be anywhere from a factor of 3 to a factor of 10. Note, however, that there is a hidden dependence on grain size and composition through the dependence of $\mathscr{T}_i$ on $x_{\rm min}$ and x_K (see eqs. [21] and [22]). $\mathscr{T}_i$ decreases for smaller $x_{\rm min}$ and x_K, and $x_{\rm min}$ decreases for smaller a, so that soft X-ray absorption becomes more important for smaller and more C-rich grains, diminishing the maximum distance at which they can be destroyed.

4.4. *UV Heating*

Finally, we compare these results to the destruction radius for UV evaporation of grains. Waxman & Draine (2000, eq. [17]) obtain a destruction radius of

$$D_{100} \approx 0.12\sqrt{\frac{L_{49}(1+0.1a_{0.1})}{a_{0.1}}} , \quad (27)$$

where $10^{49}L_{49}$ ergs s^{-1} is the total burst luminosity in photons with energies between 1 and 7.5 eV. Waxman & Draine estimate $L_{49} \approx 1$ based largely on the observed prompt emission from GRB 990123, whose optical flash now appears to have been brighter than average (Williams et al. 1999; Akerlof et al. 2000). Thus, heating by the UV-optical flash and by X-rays have roughly comparable importance for grain evaporation, and either may be more important, depending on the burst spectrum and grain size. Neither evaporation mechanism competes with grain shattering under normal circumstances.

At this point one may raise the question, "How is it that charging is able to destroy grains so much farther away from the burst than heating can? In the end, both mechanisms must supply the energy to break the same number of bonds." The answer to this question has several components. First, shattering to small sizes may still leave the grains as clusters of $\sim$100 atoms; if so, in contrast to sublimation, which transforms the grain into individual free atoms, only $\sim$1% of the bonds have been broken by the charging mechanism. Additionally, shattering exploits existing defects in grain crystalline structure, again reducing the number of bonds that must be broken to split the grain. Finally, both mechanisms have small, but different, efficiencies. Energy is wasted in the charging mechanism by giving free electrons more energy than is required to leave the grains and by the energy lost to heat when ionizations occur that do not result in electrons escaping the grain. In the case of radiative heating, even more energy is lost by radiative cooling. Thus, the contrast in effectiveness of these two mechanisms is due to the quantitative balancing of several different effects.

5. DISCUSSION: BURST AFTERGLOW EXTINCTION

Grains evaporated by the heating mechanism immediately cease to contribute anything to extinction because their material is dispersed in the gas phase. Laboratory simulations of sudden grain heating have shown that they evaporate into atoms and small molecules such as SiO (Duley & Boehlau 1986). On the other hand, when a grain is shattered by electrostatic stresses, the immediate effect is to create several new, smaller grains. As long as these pieces are large enough to act effectively as "solids," their total absorptive opacity is unchanged, but their total scattering opacity for long wavelengths is sharply diminished while their total scattering opacity for short wavelengths is increased. However, this immediate result of shattering is not the final result. As discussed in the Appendix, the total time required for successive grain shatterings to pulverize them down to very small sizes is only a modest multiple of the time required for the first break.

All of the estimates so far depend on treating the grains as macroscopic solids whose intrinsic properties are independent of size. However, as they are broken into smaller pieces, this assumption becomes questionable. It is possible, for example, that dislocations or fractures become increasingly rare as larger grains are split into smaller pieces, in part by cracking at defect sites. If so, the critical stress would increase as a decreases. On the other hand, it is also possible that the continuing irradiation by the burst and its afterglow—and the shattering events themselves—may create new lattice defects.

5.1. *Atomic Cluster Opacity*

One possible outcome, then, is that rising critical stress causes the fragmentation process to slow, and perhaps stop, as the grains reach a typical size of a few tens to hundreds of angstroms. The physics of such "atomic clusters" is unfortunately very poorly understood because neither the approximations appropriate to macroscopic solids nor those appropriate to molecules are valid in this transition regime.

We can, however, make some rough guesses about the optical behavior of a population of such small grains. In this case, the effect of dust destruction on extinction should vary strongly with wavelength because of the differing dependence of scattering and absorption efficiencies on grain size. Because the absorption efficiency of grains smaller than a wavelength scales $\propto a/\lambda$, the total absorption opacity depends only on the mass in grains, and not at all on the grain size distribution; scattering opacity, however, depends strongly on grain size. At rest-frame wavelengths greater than $\simeq$2200 Å, the dust albedo (assuming a conventional dust size distribution) is $\simeq$0.8 (Laor & Draine 1993); consequently, for these wavelengths, grain shattering reduces the total extinction by about a factor of 5. Between $\simeq$2200 and $\simeq$1400 Å the albedo falls to $\simeq$0.4, and is roughly constant from there to $\simeq$80 Å. Therefore, shattering grains to the atomic cluster scale reduces the extinction for $\lambda < 1400$ Å by only about a factor of 0.6.

5.2. *Large-Molecule Opacity*

Should the shattering process continue to operate on atomic clusters, the "grains" begin to behave more like large molecules than small solids. The issue of critical stress gradually changes to the issue of the existence of bound

states for highly charged molecular ions. UV photons, although relatively ineffective at causing electron losses in larger grains because they cannot penetrate the surface, become more efficient at ionization when the structure is only a few tens of angstroms across. The absorptive opacity, which varies comparatively smoothly with wavelength in solids, gradually becomes concentrated into a number of molecular resonances. In this subsection we discuss the effect on interstellar opacity if grain shattering results in a new population of large molecules.

It is now widely thought that a substantial fraction of the UV extinction in our own Galaxy may come from polycyclic aromatic hydrocarbons (PAHs) (cf. Li & Draine 2001). These large molecules (in some cases made up of more than a dozen benzene rings) may be a by-product of the destruction of carbonaceous grains. As absorption by PAHs is now suspected to be the primary cause of the 2200 Å feature in the Galactic extinction curve (Weingartner & Draine 2001), this feature may remain even as the carbonaceous grains are destroyed. However, there is substantial evidence that the ionizing radiation of both active galactic nuclei (Rigopoulou et al. 1999; Laurent et al. 2000) and young stars (Boselli et al. 1997) can destroy PAHs. Indeed, studies of extinction in starburst galaxies find no evidence for PAH-induced absorption (Gordon, Calzetti, & Witt 1997; Calzetti, Kinney, & Storchi-Bergmann 1994). It is therefore doubtful that the PAHs formed by the shattering of large grains could long survive the UV radiation from the burst without protection from intervening larger grains. Thus, while a PAH feature might appear during the burst, and mid-IR emission from the excited PAHs might be visible (Bauschlicher & Bakes 2000), these particles might not survive to provide long-lasting attenuation.

5.3. *Small-Molecule Opacity*

When silicate grains are destroyed, there is no large molecule analog of PAHs; instead, they may be broken into small molecules such as SiO. These molecules offer a rich UV line spectrum, and substantial enhancement of their abundance as a result of returning heavily depleted Si to the gas phase may sharply increase the equivalent width of these lines. For example, in the $E\ ^1\Sigma^+$–$X\ ^1\Sigma^+$ system of SiO there are band heads at 1924.6, 1900.2, 1876.7 Å, ... (Elander & Smith 1973). There is another potentially observable system ($J\ ^1\Pi$–$X\ ^1\Sigma^+$) whose longest-wavelength band head is at 1310.1 Å (Morton 1975). In other molecules (e.g., CO: van Dishoeck & Black 1988), some electronic transitions lead to photodissociation; if transitions like these also exist in SiO, UV absorption bands might appear for only as long as it takes the continuing UV afterglow to destroy the newly created molecules. Unfortunately, even for known bands the oscillator strengths are very uncertain (Pwa & Pottasch 1986), so it is difficult to make quantitative predictions for these features.

It is conceivable that if carbonaceous grains are broken into PAHs and silicate grains are transformed into SiO and related molecules, there might then be so many strong molecular lines as to recreate an effectively continuous opacity; however, the most astrophysically abundant elements found in grains (i.e., C and O) are not depleted by more than a factor of a few anywhere, while the next most abundant (Mg and Si) are never depleted by more than a factor of 10 (Savage & Sembach 1996). Consequently, the additional opacity created by molecules formed from destroyed grains is unlikely to increase the effective continuous opacity by a large factor.

5.4. *Atomic and Ionic Opacity*

If grain shattering releases individual atoms and ions into the ISM, species that are ordinarily strongly depleted may produce observable features. For example, in cold regions, the depletion factors for Ca, Ti, Cr, Fe, Co, and Ni range from $\sim 10^2$ to $\sim 10^4$; even in warmer regions they are depleted by factors of $\sim$10–100 (Savage & Sembach 1996). If grains are truly broken all the way to atoms and ions, these elements are returned to the gas phase, where their ability to produce absorption lines is enhanced relative to the normal circumstance in which they are locked into solid particles. Because these elements also have first ionization potentials smaller than that of O, the most abundant element in silicates (6–8 eV rather than 13.6 eV), one might expect that they will take up a disproportionate share of the charge. Therefore, immediately after the destruction of the grains these elements would be a mix of neutral atoms and singly charged ions.

The ideal lines to use as signatures of dust breakup are resonance lines in these species that fall in the rest-frame UV (so that redshifts of 1–2 make them easily observable) and have undepleted optical depths of $\sim$1–100 (so that they are easily detected if undepleted, but weak normally). The optical depth at line center is

$$\tau_{lc} \simeq 1500 f N_{21} \left(\frac{\lambda}{1000\ \text{Å}}\right)\left(\frac{b}{10\ \text{km s}^{-1}}\right)^{-1}\left(\frac{X_i}{10^{-5}}\right), \quad (28)$$

where f is the oscillator strength, N_{21} is the H column density in units of 10^{21} cm^{-2}, λ is the wavelength of the specific transition, b is the characteristic velocity width of the atoms, and X_i is the population relative to H of the ground state of the transition. From this expression we see that the lines capable of signalling dust breakup may vary from case to case (depending, for example, on b), but in many cases will have oscillator strengths rather less than unity.

Here we present a few examples of candidate lines. Because of the large number of variables that might affect any particular burst, we stress that there is no way to select a list of lines that will, in all circumstances, be the most likely to appear only when the grains along the line of sight are shattered. We concentrate on the ions Ca I, Ca II, Ti I, and Ti II because their ground states are sufficiently well separated in energy from other levels that one might reasonably expect them to contain most of the population of these ions; the spectroscopy of neutral or singly ionized Fe-group elements is so much more complicated that there is no simple way to estimate the fractional population in the lower level of any particular transition. Governed by these considerations, we have chosen, from among the many listed in Morton (1991), a few lines that might be particularly promising: Ca I λ2275; the eight-line multiplet Ti I $\lambda\lambda$2934–2951, the 11 line multiplet Ti II $\lambda\lambda$3217–3238, and the 10 line multiplet Ti II $\lambda\lambda$1895–1911. If all of each element's population were in the ground state of the species in question, the local abundances relative to H were as given by Anders & Grevesse (1989) for the solar system, and N and b had their fiducial values, the undepleted line-center optical depths for these transitions (for each line in a multiplet, but averaging over the lines within a multiplet) would be 48, 3.8, 8.5, and 2.4, respectively. Even the depletion seen

in warm regions of our own Galaxy's ISM would cause these lines to disappear, but return to the gas phase might return them to observability. If a burst were observed very soon after it begins, it might even be possible to watch a line of this sort grow in strength.

6. CONCLUSIONS

This work demonstrates that, at least under certain circumstances, X-rays emitted during and immediately after a γ-ray burst can substantially diminish extinction along the line of sight to a burst. However, as shown by both the numerous scaling parameters we employ and our discussion of the physics uncertainties, this does not necessarily happen. Given the wide dispersion in the properties of burst afterglows, not to mention the likely wide dispersion in the distribution of dust along the lines of sight to bursts, all possibilities, from null to complete elimination of extinction, may happen.

Because the X-rays are largely emitted within tens of seconds to minutes after the start of a burst, yet the optical transient may be observable well before the X-rays cease, in some cases it may be possible—if a response time of $\lesssim 1$ minute can be achieved—to watch the extinction change as the grains are destroyed. Indeed, both the strength and color of the extinction may vary, as larger grains are pulverized down to smaller grains, and as molecules and atoms are released from the dust, and sometimes ionized. We have identified several candidate spectral features that might signal these processes.

We close by noting that the physics discussed above has potential applications to other astrophysical objects. Soft gamma repeaters may destroy dust locally by the same mechanisms as GRBs. Quasars are likely to destroy dust through charging and electrostatic shattering, although their lower peak fluxes render X-ray heating and sublimation fairly ineffective except very close to the galactic nucleus. On a smaller scale, Galactic "microquasars" and X-ray binaries may similarly shatter nearby grains. These objects, with their persistent or repeating emission, may offer another useful laboratory to search for X-ray grain destruction.

We thank David Neufeld for instruction in molecular spectroscopy, Daniela Calzetti and Sangeeta Malhotra for discussions of the properties of interstellar dust, and our second referee, John Mathis, whose insightful report led to significant improvement in the clarity of this paper.

This work was partially supported by NSF grant AST 96-16922 and NASA grant NAG 5-9187 (J. H. K.). J. E. R.'s work is supported by an Institute Fellowship at The Space Telescope Science Institute (STScI), which is operated by AURA under NASA contract NAS 5-26555.

APPENDIX

THE TIME REQUIRED TO BREAK GRAINS TO MOLECULAR SIZE

As shown in Figure 1, the fluence required to break grains generally decreases with diminishing size over much of the size range between 1 and 0.01 μm, and then slowly increases as the grain size becomes still smaller. Consequently, the total fluence necessary to break "large" grains into pieces ~ 0.01 μm in size is a modest multiple of the fluence accumulated before the first break provided the critical stress does not increase greatly as a decreases. The total fluence absorbed in order to crack grains into still smaller pieces is also comparable to the fluence that produces the first break (given the shakier assumption that "solid state" behavior applies) because the dynamic range in size between the scale on which the curves "bend" and the molecular scale is not too great. The remainder of this Appendix will be devoted to quantifying these statements.

We begin by estimating the total fluence required to traverse the first part of the curve. The fundamental physical reason for the change in trend is the transition from $x_{\rm min} > x_K$ to $x_{\rm min} < x_K$. Consequently, to make this first estimate we assume that $x_{\rm min} > x_K$. To further simplify the calculation, we also make the approximations that grains break into k round pieces each time they are electrostatically shattered and that they share the charge evenly. It is conceivable that in grains with good electrical conductivity (e.g., those made of graphite) the charge would all migrate to the surface and that this surface layer might break off, leaving a remnant almost as large as the original grain. However, in addition to the requirement on the electrical conductivity, this process would also require any imperfections in the grain lattice structure to concentrate near the surface. We view this combination of prerequisites as unlikely. Finally, for convenience of discussion, we also assume that the X-ray flux is constant during the time that it is "on," so that time is proportional to fluence.

From equation (14), we see that there is a critical charge for shattering grains,

$$Z_{g,\rm crit} = 7.5 \times 10^4 a_{0.1}^2 S_{\rm crit,10}^{1/2} . \tag{A1}$$

Combining all the scaling factors except those involving x_K and a into one constant D, the time to reach this critical charge starting from $Z_g = 0$ is then

$$t_{\rm break}^0 \simeq 4^{3+\alpha} D x_K^{-3} a_{0.1}^{1+2\alpha/3} . \tag{A2}$$

So long as $\alpha > -3/2$ ($-1 < \alpha < 1$ is the usual range), $t_{\rm break}$ does indeed decline with decreasing a. We now rewrite the breaking time in terms of how many shattering events were required to reach that size. Using the assumption of even breaking into round pieces, the size of the fragments after m breaks is $a_m = a_o k^{-m/3}$ (with a_o the original grain size). If these fragments were born with no charge, the X-ray irradiation time to break them the $(m+1)$th time would be

$$t_{\rm break}^m \simeq t_{\rm break}^0 k^{-m(1+2\alpha/3)/3} . \tag{A3}$$

In fact, the true time to reach the breaking point is somewhat smaller because each piece inherits its share of the charge on the original grain. Using the relation $a_m = a_o k^{-m/3}$ in equation (A1), we see that the charge per fragment required to produce the $(m+1)$th break is $\propto k^{-2m/3}$. If this is divided evenly among the successor fragments, each one acquires a charge $\propto k^{-2m/3-1}$. But the charge required to shatter this next generation is $\propto k^{-2(m+1)/3}$, so the fraction of the required charge

with which the fragments are born is $k^{-1/3}$. Thus, the fluence necessary to reach the critical stress the next time is reduced by the factor $1 - k^{-1/3}$, a quantity that could be anywhere from, say, $\simeq 0.2$ (for $k = 2$) to $\simeq 0.5$ (for $k = 10$).

Combining this correction factor with the estimate for $t_{\rm break}$, we find that the total time between the initiation of the X-ray irradiation and the time of the Mth fracture is

$$t_{tot}^{M} \simeq t_{\rm break}^{0}\left[1 + (1 - k^{-1/3}) \sum_{m=1}^{M} k^{-m(1+2\alpha/3)/3}\right]. \tag{A4}$$

This is a convergent series. In the limit $M \gg 1$, the result approaches

$$t_{tot}^{\infty} \simeq t_{\rm break}^{0}\left[1 + \frac{1 - k^{-1/3}}{k^{(1+2\alpha/3)/3} - 1}\right], \tag{A5}$$

which exceeds $t_{\rm break}^{0}$ by a modest factor. For example, when $\alpha = 0$, the total time is simply $1 + k^{-1/3}$ times the time required for the first break.

Although the approximation $x_{\rm min} > x_K$ is broadly valid, it is not universally applicable. In carbon-rich grains, for which $x_K = 0.28$, it is a valid approximation for fragments as small as $\simeq 18$ Å. Grains this small are hardly more than large molecules, so the expressions just derived apply well to the entire destruction process for carbon-rich grains.

However, in silicate grains, for which $\langle x_K^3 \rangle \simeq 1$, the approximation $x_{\rm min} > x_K$ is only appropriate for $a \gtrsim 0.013$ μm = 130 Å. For smaller grains, $x_K > x_{\rm min}$, and the nominal breaking time then becomes

$$t_{\rm break} = D x_K^{\alpha} a_{0.1}^{-1} \ ; \tag{A6}$$

that is, the breaking time actually *increases* as the grain becomes smaller. This is because the charging rate is proportional to the volume of the grain ($\propto a^3$), whereas the critical charge is $\propto a^2$. Consequently, the total time to break silicate grains is however long it takes to reach the $x_{\rm min} < x_K$ regime plus an additional time

$$t_{*} \simeq D x_K^{\alpha} a_{o,0.1}^{-1} (1 - k^{-1/3}) \sum_{m=m_{*}+1}^{M} k^{m/3} \ , \tag{A7}$$

where $a_{o,0.1}$ is the original grain size in units of 0.1 μm and m_{*} is the number of breaks necessary to reduce the grain to a size such that $x_{\rm min} < x_K$. The sum in equation (A7) is $(k^{M/3} - k^{m_{*}/3})/(1 - k^{-1/3})$; therefore,

$$t_{*} \simeq D x_K^{\alpha} a_{o,0.1}^{-1} (k^{M/3} - k^{m_{*}/3}) \ . \tag{A8}$$

Here the two critical numbers of events are

$$m_{*} = 3 \log_k (7.7 a_{o,0.1} x_K^{-3/2}) \ , \tag{A9}$$

$$M \simeq 3 \log_k (33 a_{o,0.1}) \ , \tag{A10}$$

where we have, in equation (A10), assumed that complete breakdown of a grain occurs when it has been reduced to 30 Å in size. For example, if we take $k = 3$, $m_{*} \simeq 6 + \log_3 (a_{o,0.1}/x_K^{3/2})$ and $M \simeq 10 + \log_3 a_{o,0.1}$. The factor $k^{M/3} - k^{m_{*}/3}$ is then $(33 - 7.7 x_K^{-3/2}) a_{o,0.1}$. Although this is a relatively large number, the absence of the $4^{3+\alpha}$ factor from t_{*} (as contrasted with $t_{\rm tot}$) means that the time spent in the $x_{\rm min} < x_K$ regime can at most be comparable to the time required for the initial break of a grain with $a \sim 0.1$ μm.

REFERENCES

Akerlof, C. W., et al. 1999, Nature, 398, 400
———. 2000, ApJ, 532, L25
Anders, E., & Grevesse, N. 1989, Geochim. Cosmochim. Acta, 53, 197
Band, D., et al. 1993, ApJ, 413, 281
Bauschlicher, C. W., & Bakes, E. L. O. 2000, Chem. Phys., 262, 285
Bloom, J. S., Djorgovski, S. G., Kulkarni, S. R., & Frail, D. A. 1998, ApJ, 507, L25
Bloom, J. S., et al. 1999a, ApJ, 518, L1
———. 1999b, Nature, 401, 453
Boselli, A., et al. 1997, A&A, 324, L13
Burke, J. R., & Silk, J. 1974, ApJ, 190, 1
Calzetti, D., Kinney, A. L., & Storchi-Bergmann, T. 1994, ApJ, 429, 582
Dal Fiume, D., et al. 2000, A&A, 355, 454
Djorgovski, S. G., et al. 1998, ApJ, 508, L17
Draine, B. T. 2000, ApJ, 532, 273
Draine, B. T., & Lee, H. M. 1984, ApJ, 285, 89
Draine, B. T., & Salpeter, E. E. 1979, ApJ, 231, 77
Duley, W. W., & Boehlau, E. 1986, MNRAS, 221, 659
Dwek, E., & Smith, R. K. 1996, ApJ, 459, 686
Elander, N., & Smith, W. H. 1973, ApJ, 184, 311
Frontera, F., et al. 2000, ApJS, 127, 59
Fruchter, A. S. 1999, ApJ, 512, L1
Fruchter, A. S., et al. 1999, ApJ, 519, L13
Galama, T. J., & Wijers, R. A. M. J. 2001, ApJ, 549, L209
Galama, T. J., et al. 1999, Nature, 398, 394
Galama, T. J., et al. 2000, ApJ, 536, 185
Gordon, K. D., Calzetti, D., & Witt, A. N. 1997, ApJ, 487, 625
Groot, P. J., et al. 1998, ApJ, 493, L27
Guhathakurta, P., & Draine, B. T. ApJ, 345, 1989, 230
Hogg, D. W., & Fruchter, A. S. 1999, ApJ, 520, 54
Katz, J. I. 1994, ApJ, 422, 248
Kouveliotou, C., Meegan, C. A., Fishman, G. J., Bhat, N. P., Briggs, M. S., Koshut, T. M., Paciesas, W. S., & Pendleton, G. N. 1993, ApJ, 413, L101
Krolik, J. H., & Kallman, T. R. 1984, ApJ, 286, 366
Laor, A., & Draine, B. T. 1993, ApJ, 402, 441
Laurent, O., Mirabel, I. F., Charmandaris, V., Gallais, P., Madden, S. C., Sauvage, M., Vigroux, L., & Cesarsky, C. 2000, A&A, 359, 887
Li, A., & Draine, B. T. 2001, ApJ, 554, 778
Mao, S., & Mo, H. J. 1998, A&A, 339, L1
Mathis, J. S. 1996, ApJ, 472, 643
———. 1998, ApJ, 497, 824
Meszaros, P., & Rees, M. J. 1997, ApJ, 476, 232
Metzger, M. R., Djorgovski, S. G., Kulkarni, S. R., Steidel, C. C., Adelberger, K. L., Frail, D. A., Costa, E., & Frontera, F. 1997, Nature, 387, 879
Morrison, R., & McCammon, D. 1983, ApJ, 270, 119
Morton, D. C. 1975, ApJ, 197, 85
———. 1991, ApJS, 77, 119
Paczyński, B., & Rhoads, J. E. 1993, ApJ, 418, L5
Pwa, T. H., & Pottasch, S. R. 1986, A&A, 164, 116

Reichart, D. E., et al. 1999, ApJ, 517, 692
Rigopoulou, D., Spoon, H. W. W., Genzel, R., Lutz, D., Moorwood, A. F. M., & Tran, Q. D. 1999, AJ, 118, 2625
Sari, R., Piran, T., & Narayan, R. 1998, ApJ, 497, L17
Savage, B., & Sembach, K. 1996, ARA&A, 34, 279
Spitzer, L. 1978, Physical Processes in the Interstellar Medium (New York: Wiley)
van Dishoeck, E. F., & Black, J. H. 1988, ApJ, 334, 771
Verner, D. A., & Yakovlev, D. G. 1995, A&AS, 109, 125
Vreeswijk, P. M., et al. 1999, ApJ, 523, 171
———. 2001, ApJ, 546, 672
Waters, L. B. F. M., et al. 1996, A&A, 315, L361
Waxman, E., & Draine, B. T. 2000, ApJ, 537, 796
Weingartner, J. C., & Draine, B. T. 2001, ApJ, 548, 296
Williams, G. G., et al. 1999, preprint (astro-ph/9912402)